PCCP

ROYAL SOCIETY OF CHEMISTRY

PAPER

View Article Online
View Journal | View Issue

Cite this: *Phys. Chem. Chem. Phys.*, 2024, **26**, 12483

Systematic analysis of electronic barrier heights and widths for concerted proton transfer in cyclic hydrogen bonded clusters: $(HF)_n$, $(HCl)_n$ and $(H_2O)_n$ where n = 3, 4, 5†

Yuan Xue, [a] Thomas More Sexton, [b] Johnny Yang ‡[a] and Gregory S. Tschumper *[a]

The MP2 and CCSD(T) methods are paired with correlation consistent basis sets as large as aug-cc-pVQZ to optimize the structures of the cyclic minima for $(HF)_n$, $(HCl)_n$ and $(H_2O)_n$ where n = 3–5, as well as the corresponding transition states (TSs) for concerted proton transfer (CPT). MP2 and CCSD(T) harmonic vibrational frequencies confirm the nature of each minimum and TS. Both conventional and explicitly correlated CCSD(T) computations are employed to assess the electronic dissociation energies and barrier heights for CPT near the complete basis (CBS) limit for all 9 clusters. Results for $(HF)_n$ are consistent with prior studies identifying C_{nh} and D_{nh} point group symmetry for the minima and TSs, respectively. Our computations also confirm that CPT proceeds through C_s TS structures for the C_1 minima of $(H_2O)_3$ and $(H_2O)_5$, whereas the process goes through a TS with D_{2d} symmetry for the S_4 global minimum of $(H_2O)_4$. This work corroborates earlier findings that the minima for $(HCl)_3$, $(HCl)_4$ and $(HCl)_5$ have C_{3h}, S_4 and C_1 point group symmetry, respectively, and that the C_{nh} structures are not minima for n = 4 and 5. Moreover, our computations show the TSs for CPT in $(HCl)_3$, $(HCl)_4$ and $(HCl)_5$ have D_{3h}, D_{2d}, and C_2 point group symmetry, respectively. At the CCSD(T) CBS limit, $(HF)_4$ and $(HF)_5$ have the smallest electronic barrier heights for CPT (≈15 kcal mol^{-1} for both), followed by the HF trimer (≈21 kcal mol^{-1}). The barriers are appreciably higher for the other clusters (around 27 kcal mol^{-1} for $(H_2O)_4$ and $(HCl)_3$; roughly 30 kcal mol^{-1} for $(H_2O)_3$, $(H_2O)_5$ and $(HCl)_4$; up to 38 kcal mol^{-1} for $(HCl)_5$). At the CBS limit, MP2 significantly underestimates the CCSD(T) barrier heights (*e.g.*, by *ca.* 2, 4 and 7 kcal mol^{-1} for the pentamers of HF, H_2O and HCl, respectively), whereas CCSD overestimates these barriers by roughly the same magnitude. Scaling the barrier heights and dissociation energies by the number of fragments in the cluster reveals strong linear relationships between the two quantities and with the magnitudes of the imaginary vibrational frequency for the TSs.

Received 29th January 2024,
Accepted 26th March 2024

DOI: 10.1039/d4cp00422a

rsc.li/pccp

1 Introduction

Double proton transfer reactions have been extensively studied due their importance in biochemistry, atmospheric chemistry, electrochemistry and other areas.[1–6] These processes can occur in a step-wise or concerted manner,[7–12] and they are often directed along pathways associated with intra- or intermolecular hydrogen bonds, such as those found in porphyrins, porphycenes, carboxylic acid dimers, nucleic acid base pairs and related systems.[13–20] In a similar manner, cyclic hydrogen bonding arrangements in trimers, tetramers, *etc.* can provide alignments conducive to analogous transfer phenomena involving three or more protons. Higher-order (triple, quadruple, *etc.*) proton transfer reactions have been characterized experimentally,[21–27] but such observations remain relatively rare compared to their double proton transfer counterparts.

Small homogeneous hydrogen-bonded clusters have provided very useful prototypes for the computational and theoretical characterization of H^+ transfer reactions involving three or more protons. When these H atoms are covalently bonded to an atom or small functional group with an appreciable electron withdrawing character and the capacity to accept a hydrogen

[a] *Department of Chemistry and Biochemistry, University of Mississippi, University, MS 38677-1848, USA. E-mail: yxue@olemiss.edu, jyang288@gmail.com, tschumpr@olemiss.edu*

[b] *School of Arts and Sciences, Chemistry University of Mary, Bismark, ND 58504, USA. E-mail: tmsexton@umary.edu*

† Electronic supplementary information (ESI) available. See DOI: https://doi.org/10.1039/d4cp00422a

‡ Current address: School of Medicine, University of Mississippi Medical Center, Jackson, MS 39202, USA.

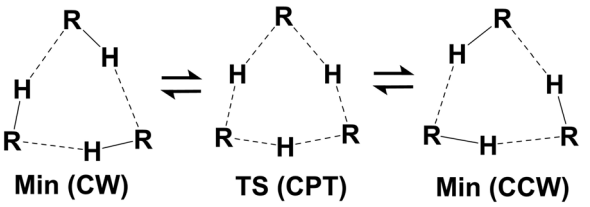

Fig. 1 General scheme for concerted proton transfer (CPT) between equivalent minima of a cyclic trimer that differ only by the relative direction of the hydrogen bonding network: clockwise (CW) *vs.* counter clockwise (CCW).

bond (R = F, Cl, OH, OCH_3, OCH_2CH_3, *etc.*), the resulting hydrogen bonded $(HR)_n$ clusters tend to adopt homodromic cyclic arrangements for $n = 3$ to $n \approx 5$ where the hydrogen bonds adopt the same relative orientation in the ring, clockwise (CW) or counter clockwise (CCW). Both scenarios are depicted in Fig. 1 for a trimer, $(HR)_3$. In this type of cyclic hydrogen-bonded network, concerted proton transfer (CPT) can occur with each fragment serving as a proton donor to one nearest neighbor while simultaneously acting as a proton acceptor from the other adjacent fragment. In the transition state (TS) associated with this CPT process (center of Fig. 1), there is an energetic barrier (ΔE^*) on the Born–Oppenheimer potential energy surface that must be overcome in the classical limit as three covalent R–H bonds are broken and three new covalent R–H bonds begin to form as an equivalent global minimum is produced (right side of Fig. 1). The two minima differ only in the relative orientation of the hydrogen bonding network. The heights and widths of these barriers, along with other features of the surface near the TS, influence the extent to which quantum mechanical tunneling occurs in these CPT processes under various conditions.

With only 2 atoms and 10 electrons per fragment, small hydrogen fluoride clusters (*e.g.*, $(HF)_n$ where $n = 3$–6) have been extensively studied in this context because they are amenable to sophisticated theoretical interrogation.[28–40] Additionally, HF clusters also exhibit rather strong and highly cooperative hydrogen bonding interactions,[38,39,41–62] and there is evidence of rapid monomer dissociation in the gas phase.[63,64] For the HF trimer, tetramer and pentamer, the H nuclei are symmetry equivalent, and proton transfer is a synchronous process that proceeds through $D_{n\mathrm{h}}$ TS structures that connect equivalent $C_{n\mathrm{h}}$ minima with electronic barrier heights (ΔE^*) estimated to be around 21, 15 and 17 kcal mol^{-1} ($\pm$2 kcal mol^{-1}) for $n = 3$, 4, 5, respectively, near the CCSD(T) complete basis set (CBS) limit.[35]

Although homogeneous hydrogen chloride trimers, tetramers and pentamers offer closely related platforms for studying hydrogen bonding,[65–75] we are aware of only a single study that has examined CPT in $(HCl)_3$.[31] As with $(HF)_3$, a synchronous process connects equivalent $C_{3\mathrm{h}}$ minima for $(HCl)_3$ through a $D_{3\mathrm{h}}$ TS, but the electronic barrier (ΔE^*) is approximately 4 to 9 kcal mol^{-1} larger based on their MP2, MP3, MP4, QCISD and QCISD(T) computations with split-valence triple-ζ basis sets.

The analogous CPT processes have also been studied in small water clusters, $(H_2O)_{n=3-5}$.[33,76–80] However, the small tunneling splittings observed in the vibration–rotation-tunneling (VRT) spectra of these cyclic water clusters are typically interpreted as tunneling through much lower barriers[81–98] associated with mechanisms that might, for example, break/form one or more weak intermolecular bonds (hydrogen bond exchange). Consequently, the high-barrier saddle points associated with CPT in small cyclic water clusters[33,76,77] have not been subjected to the same rigorous analyses used to characterize the analogous proton transfer processes in cyclic hydrogen fluoride clusters. Nevertheless, a direct experimental observation of concerted proton tunneling of $(H_2O)_4$ on a Au-supported NaCl(001) film was reported in 2015, and the experiments revealed that the process could be suppressed or enhanced by a Cl-terminated scanning tunneling microscope tip.[27] Additionally, a delocalized proton model has also shown that similar tunneling processes in the cyclic H_2O trimer[99] and pentamer[100] are consistent with the 2-dimensional IR spectrum of liquid water[101] and can also reproduce the splitting patterns in the VRT spectra of $(H_2O)_3$ and $(H_2O)_5$.

In light of the fundamental importance of CPT processes in these small cyclic hydrogen bonded clusters and some relatively large uncertainties in the associated barrier heights, the present study was initiated to rigorously characterize the minima and corresponding TS structures of $(HF)_n$, $(HCl)_n$ and $(H_2O)_n$ clusters, where $n = 3$, 4, 5, with conventional and explicitly correlated CCSD(T) computations. All of the structures were optimized with the MP2 and CCSD(T) methods utilizing triple- and quadruple-ζ correlation consistent basis sets augmented with diffuse functions. Harmonic vibrational frequencies were also computed to confirm the nature of each stationary point and gauge the width of the barriers near at each TS from the magnitude of the imaginary vibrational frequency. The electronic barrier heights (ΔE^*) for CPT near the complete basis set (CBS) limit are estimated from both extrapolation techniques and explicitly correlated computations. To the best of our knowledge, this work reports the first characterization of the TSs for CPT in $(HCl)_4$ and $(HCl)_5$. The data reported here not only provide important benchmark structures, energetics and vibrational frequencies for these systems, but they also enable direct comparison of the barriers for CPT between $(HF)_n$, $(HCl)_n$ and $(H_2O)_n$ for $n = 3$, 4, 5.

2 Computational methods

The structures of the global minima and CPT TSs for $(HF)_n$, $(HCl)_n$ and $(H_2O)_n$ for $n = 3$, 4, 5 were fully optimized along with a few higher-order saddle points and the isolated HF, HCl, and H_2O monomers using the MP2[102] and CCSD(T)[103–105] *ab initio* quantum mechanical electronic structure methods in conjunction with correlation consistent basis sets augmented with diffuse functions on all atoms[106–108] (aug-cc-pV*X*Z where *X* = D, T, Q and abbreviated here as a*X*Z). The corresponding harmonic vibrational frequencies were also computed to confirm the number and nature of imaginary vibrational frequencies associated with each stationary point (although this was

not feasible with the CCSD(T) method and aQZ basis for some of the pentamer structures). Gradients were evaluated analytically except for the CCSD(T)/aQZ geometry optimizations of the $(H_2O)_5$ structures which employed finite difference procedures. Residual components of the gradient for the optimized structures did not exceed 1×10^{-6} E_h/a_0 in the former case and did not exceed 5×10^{-5} E_h/a_0 for the latter scenario. For most frequency computations, the Hessians were also obtained analytically. However, CCSD(T) harmonic frequencies were evaluated *via* finite differences of gradients for some of the larger clusters and some of the computations with the the aQZ basis set.

The barrier heights for CPT (ΔE^*) were calculated directly from the differences in total electronic energies of the corresponding minima and TS structures for each cluster. In a similar manner, the electronic dissociation energies (ΔE) of the $(HF)_n$, $(HCl)_n$ and $(H_2O)_n$ for n = 3, 4, 5 global minima were determined from the energy difference between the cluster and n times the energy of an isolated monomer. Although this approach to evaluating ΔE introduces a basis set superposition inconsistency,[109,110] the popular counterpoise (CP) procedure[111,112] was not implemented because the discrepancy vanishes by definition at the complete basis set (CBS) limit.

Additional single point energy computations were carried out on the CCSD(T)/aQZ optimized structures to determine ΔE and ΔE^* near the CBS limit. Conventional CCSD(T) energies were computed with the aTZ, aQZ, a5Z and a6Z basis sets was well as their counterparts that only add diffuse functions to the heavier non-hydrogen atoms (*i.e.* cc-pV*X*Z for H and aug-cc-pV*X*Z for O, F and Cl, hereafter denoted ha*X*Z). Estimates of the Hartree–Fock self-consistent field energy at the CBS limit (E_{SCF}^{CBS}) was obtained using an algebraic expression[113] for the three-parameter exponential function proposed by Feller[114] with energies from 3 sequential basis sets (small (SZ), medium (MZ) and large (LZ), such as aTZ/aQZ/a5Z or haQZ/ha5Z/ha6Z).

$$E_{SCF}^{CBS} = E_{SCF}^{LZ} - \frac{\left(E_{SCF}^{LZ} - E_{SCF}^{MZ}\right)^2}{E_{SCF}^{SZ} - 2E_{SCF}^{MZ} + E_{SCF}^{LZ}} \quad (1)$$

Similarly, the electronic correlation energy at the CBS limit (E_c^{CBS}) was calculated using an algebraic expression[113] for the two-parameter inverse cubic function described by Helgaker and co-workers[115] with two consecutive basis sets from either the a*X*Z or ha*X*Z series (denoted here as *s*Z and *l*Z for the smaller and larger basis sets, respectively).

$$E_c^{CBS} = \frac{l^3 E_c^{lZ} - s^3 E_c^{sZ}}{l^3 - s^3} \quad (2)$$

Independent estimates of electronic energies for the CCSD(T)/aQZ optimized structures near the CBS limit were also obtained from explicitly correlated CCSD and CCSD(T) computations[116–119] carried out with the corresponding a*X*Z-F12 and ha*X*Z-F12 families of basis sets (X = D, T, Q, 5).[120,121] The results reported here were obtained with ansatz F12b and default auxiliary basis sets in the Molpro 2022 quantum chemistry program,[122–124] and the triples contributions were not scaled. These computations also provide density fitted explicitly correlated MP2 (DF-MP2-F12) electronic energies, with the fixed amplitude ansatz 3C, that are used to estimate energetics near the MP2 CBS limit along with the aforementioned extrapolations.

All MP2 optimizations and frequency computations were performed with the Gaussian16 software package.[125] Most conventional CCSD(T) computations were performed with the CFOUR suite of quantum chemistry programs,[126,127] although some of the energies and analytical gradients were obtained with Molpro 2022. A frozen-core approximation was employed for all computations that excluded the 1s-like orbitals of fluorine and oxygen as well the 1s-, 2s-, and 2p-like orbitals of chlorine from the electron correlation procedures.

3 Results and discussion

3.1 Structures of minima and transition states

The structures optimized in this investigation for the minima and TSs of the HF and H_2O clusters are consistent with those reported in previous studies (see the introduction and references therein). For the $(HF)_n$ clusters, the minima are planar with C_{nh} point group symmetry (top row of Fig. 2), whereas the TSs associated with the CPT processes have D_{nh} symmetry (bottom row of Fig. 2). For the $(H_2O)_n$ clusters, the minima have C_1, S_4, and C_1 point group symmetry for n = 3, 4, 5, respectively, and their structures are shown in the top row of Fig. 3. The corresponding TS structures for CPT can be seen in the bottom row of the figure, and they are somewhat more symmetric with D_{2d} point group symmetry for the tetramer and C_s point group symmetry for the trimer and pentamer. An analogous D_{2d} TS structure for CPT also connects equivalent S_4 minima in the methanol tetramer.[128]

The cyclic minima of $(HCl)_{n=3,4,5}$ have been less thoroughly characterized than those of $(HF)_n$ and $(H_2O)_n$. Nevertheless, our MP2 and CCSD(T) optimized structures shown in the top row of Fig. 4 are consistent with prior studies of these clusters using comparable methods and basis sets.[71,73,75,129] Although the HCl trimer adopts the same C_{3h} configuration as $(HF)_3$, the cyclic minima for the HCl tetramer and HCl pentamer are not planar and exhibit hydrogen bond configurations that more closely resemble those of $(H_2O)_4$ and $(H_2O)_5$. Our MP2 and CCSD(T) computations with the aDZ, aTZ and aQZ basis sets indicate that the planar C_{4h} structure of $(HCl)_4$ has 1 small imaginary frequency and is slightly higher in energy than the puckered S_4 minimum (within 0.1 kcal mol^{-1}). For the HCl pentamer, the cyclic minimum is also non-planar with C_1 symmetry. Moreover, the present investigation has identified three TS structures for CPT in the cyclic HCl trimer, tetramer and pentamer (bottom row of Fig. 4), which are reported here for the first time, to the best of our knowledge, for n = 4 and 5. The TS is planar with D_{3h} symmetry for $(HCl)_3$, puckered with D_{2d} symmetry for $(HCl)_4$ and non-planar with C_2 symmetry for $(HCl)_5$.

Although multiple covalent bonds are broken in the CPT processes being studied here, the single-reference nature of the

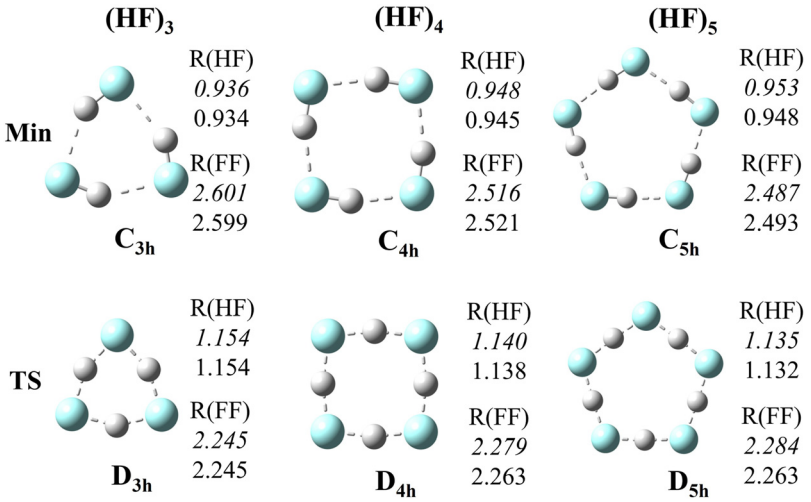

Fig. 2 Structures and point group symmetries (in bold) of the $(HF)_{n=3,4,5}$ minima (top row) and transition states (bottom row) along with select interatomic distances (R(HF) and R(FF) in Å) from MP2/aQZ (in italics) CCSD(T)/aQZ optimizations, with the Cartesian coordinates provided in the ESI† (Tables S1–S6).

TS structures was noted in one of the earliest studies of these systems. The 1991 *ab initio* study of CPT in water clusters by Garrett and Melius[76] stated that preliminary MCSCF computations "on the transition-state structure of the cyclic water trimer indicate that the electronic structure is dominated by a single configuration." Early work on CPT in $(HF)_{n=3,4,5}$ clusters also pointed out that a multiconfiguration treatment was not necessary[77] based on the small T_1 diagnostic reported for the HF trimer from CCSD(T) computations by Komornicki, Dixon and Taylor, "which would indicate that nondynamical correlation effects should not be a problem."[30] Our own CCSD(T)/aQZ computations show that both the T_1 and D_1 diagnostics[130–133] are small, with values for the TS structures being only slightly larger than those for the corresponding minima ($T_1 \leq 0.010$ for all minima and ≤ 0.011 for all TS structures; $D_1 \leq 0.023$ for all minima and ≤ 0.025 for all TS structures).

3.2 Harmonic vibrational frequencies

MP2 and CCSD(T) harmonic vibrational frequencies (ω) were also computed for the 9 minima and 9 transition states described in the previous section (Tables S19–S36 in the ESI†). For the minima, the intramolecular stretching frequencies associated with the hydrogen bond network are reported in Tables 1–3 along with the corresponding monomer stretching frequencies.

It is well known that hydrogen bonding significantly perturbs these stretching frequencies to lower energies ($\Delta\omega$). The effect is most pronounced in the $(HF)_n$ clusters and least

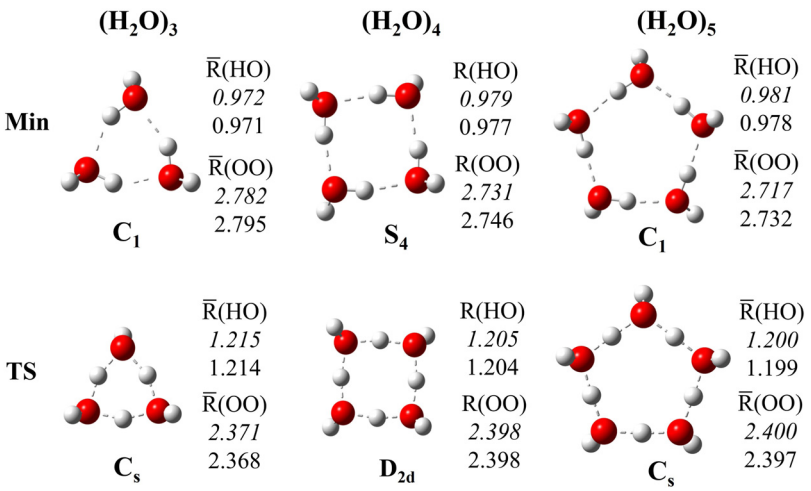

Fig. 3 Structures and point group symmetries (in bold) of the $(H_2O)_{n=3,4,5}$ minima (top row) and transition states (bottom row) along with select interatomic distances (R(HO) and R(OO) in Å) for n = 4 and average interatomic distances ($\bar{R}$(HO) and $\bar{R}$(OO) in Å) for n = 3, 5 from MP2/aQZ (in italics) CCSD(T)/aQZ optimizations, with the Cartesian coordinates provided in the ESI† (Tables S7–S12).

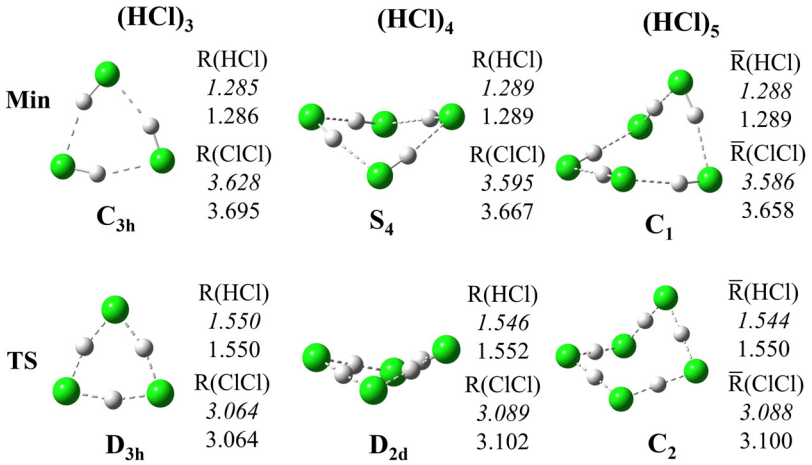

Fig. 4 Structures and point group symmetries (in bold) of the $(HCl)_{n=3,4,5}$ minima (top row) and transition states (bottom row) along with select interatomic distances (R(HCl) and R(ClCl) in Å) for n = 3, 4 or average interatomic distances ($\bar{R}$(HCl) and $\bar{R}$(ClCl) in Å) for n = 5 from MP2/aQZ (in italics) CCSD(T)/aQZ optimizations, with the Cartesian coordinates provided in the ESI† (Tables S13–S18).

pronounced in the $(HCl)_n$ systems. The CCSD(T) computations with the aTZ basis set show that the HF stretching frequencies decrease by nearly 400 cm^{-1} relative to the monomer for $(HF)_3$ and that the maximum shifts ($\Delta\omega_{max}$) increase in magnitude with the size of the cluster to more than 800 cm^{-1} for $(HF)_5$. For $(H_2O)_n$, the CCSD(T)/aTZ shifts grow with n from around −200 cm^{-1} for n = 3 to nearly −400 cm^{-1} for n = 5 (for the OH stretching frequencies associated with the hydrogen bonds relative to the symmetric OH stretching frequency of the monomer). Although the HCl stretching frequencies decrease by more than 100 cm^{-1} in the trimer, the magnitudes of the shifts do not increase significantly for n = 4 or 5 (<50 cm^{-1} at the CCSD(T)/aTZ level of theory).

In the six clusters with C_{nh} or S_4 point group symmetry ($(HF)_{n=3,4,5}$, $(H_2O)_4$, $(HCl)_{n=3,4}$), the $\Delta\omega_{max}$ values in Tables 1–3 are associated with the totally symmetric intrafragment stretching mode of the H atoms in the hydrogen bond network. Although these in-phase modes are IR inactive, they are accessible *via* complimentary Raman spectroscopy measurements, and their coupling with the out-of-phase modes is sensitive to many-body effects that could also influence multiple proton tunneling.[134] A similar situation is observed for the 3 minima with C_1 point group symmetry ($(H_2O)_{n=3,5}$ and $(HCl)_5$). The corresponding pseudo symmetric stretching modes have the lowest harmonic vibrational frequencies (ω) and consequently give the largest magnitude shifts ($\Delta\omega_{max}$). These modes have sizable Raman scattering activities, and although their IR intensities are no longer formally zero within the double harmonic approximation due to symmetry, the intensities remain very small.

In all cases, MP2 appreciably overestimates the magnitudes of these $\Delta\omega$ shifts relative to the corresponding CCSD(T) results (*e.g.*, by 38 to 92 cm^{-1} with the aTZ basis set). Like $(HF)_2$ and $(H_2O)_2$,[135] the basis set convergence of the harmonic vibrational frequencies for these cyclic HF and H_2O clusters is not necessarily monotonic (Tables S19–S36 in the ESI†) but fairly rapid for most intramolecular modes.

Table 1 Harmonic HF stretching frequencies (ω in cm^{-1} and labelled by irreducible representations) for the $(HF)_{n=3,4,5}$ minima along with the maximum frequency shifts relative to the HF monomer induced by the hydrogen bond network ($\Delta\omega_{max}$)

	MP2			CCSD(T)		
	aDZ	aTZ	aQZ	aDZ	aTZ	aQZ
HF						
$\omega(\sigma^+)$	4082	4123	4137	4081	4125	4142
$(HF)_3$						
$\omega(e')$	3782	3832	3838	3809	3864	3872
$\omega(a')$	3665	3711	3716	3700	3751	3758
$\Delta\omega_{max}$	−418	−411	−421	−381	−373	−384
$(HF)_4$						
$\omega(b_g)$	3602	3638	3656	3652	3694	3712
$\omega(e_u)$	3527	3556	3576	3583	3618	3638
$\omega(a_g)$	3333	3348	3374	3403	3426	3452
$\Delta\omega_{max}$	−749	−775	−763	−677	−699	−690
$(HF)_5$						
$\omega(e_2')$	3529	3545	3570	3587	3611	3636
$\omega(e_1')$	3413	3417	3447	3479	3492	3522
$\omega(a')$	3213	3197	3238	3296	3290	3331
$\Delta\omega_{max}$	−870	−926	−900	−784	−834	−811

The imaginary harmonic vibrational frequencies (ω_i) associated with the TS structures for CPT in each cluster are tabulated in Table 4, and they provide information about the widths of the barriers associated with the proton transfer process. For each value of n, the magnitude is consistently largest for $(H_2O)_n$, with the CCSD(T)/aTZ values decreasing monotonically from 1915i cm^{-1} for the trimer to 1724i cm^{-1} for the pentamer. In contrast, the cluster with the smallest magnitude for ω_i changes from $(HCl)_n$ for n = 3 to $(HF)_n$ for n = 4, 5 (1652i, 1515i and 1433i cm^{-1}, respectively, at the CCSD(T)/aTZ level of theory). The MP2 computations consistently underestimate the magnitude of the CCSD(T) imaginary frequencies (by *ca.* 90 cm^{-1} for $(HF)_n$, 110 cm^{-1} for $(H_2O)_n$ and 150 cm^{-1} for $(HCl)_n$ with the aug-cc-pVTZ basis set). The computed

Table 2 Harmonic bound OH stretching frequencies (ω in cm^{-1} and labelled by irreducible representations) for the $(H_2O)_{n=3,4,5}$ minima along with the maximum frequency shifts relative to the $\omega(a_1)$ symmetric OH stretching frequency of the H_2O monomer induced by the hydrogen bond network ($\Delta\omega_{max}$)

	MP2			CCSD(T)		
	aDZ	aTZ	aQZ	aDZ	aTZ	aQZ
H_2O						
$\omega(b_2)$	3938	3948	3966	3905	3920	3941
$\omega(a_1)$	3803	3822	3840	3787	3811	3831
$(H_2O)_3$						
ω(a)	3641	3650	3664	3655	3669	3685
ω(a)	3633	3641	3654	3648	3662	3678
ω(a)	3575	3578	3591	3597	3605	3621
$\Delta\omega_{max}$	−229	−244	−248	−190	−206	−210
$(H_2O)_4$						
ω(b)	3524	3530	3545	3559	3570	3588
ω(e)	3486	3490	3506	3527	3534	3554
ω(a)	3396	3393	3412	3447	3448	3471
$\Delta\omega_{max}$	−408	−428	−428	−340	−363	−360
$(H_2O)_5$						
ω(a)	3494	3499	3515	3535	3544	—
ω(a)	3487	3490	3507	3530	3537	—
ω(a)	3442	3443	3461	3490	3495	—
ω(a)	3433	3434	3451	3483	3487	—
ω(a)	3354	3350	3370	3413	3413	—
$\Delta\omega_{max}$	−450	−471	−470	−374	−398	

imaginary frequencies also exhibit appreciable basis set sensitivity for the $(HF)_n$ clusters with the aTZ results being smaller in magnitude than the aQZ values by approximately 30, 50 and 60 cm^{-1} for n = 3, 4, 5, respectively. The differences between the aTZ and aQZ results are smaller for the $(H_2O)_n$ and $(HCl)_n$ clusters (typically *ca.* 20 cm^{-1}). Although the relative magnitudes stay the same for H_2O (aTZ values larger than aQZ), they reverse for HCl (aTZ values smaller than aQZ).

Table 3 Harmonic HCl stretching frequencies (ω in cm^{-1} and labelled by irreducible representations) for the $(HCl)_{n=3,4,5}$ minima along with the maximum frequency shifts relative to the HCl monomer induced by the hydrogen bond network ($\Delta\omega_{max}$)

	MP2			CCSD(T)		
	aDZ	aTZ	aQZ	aDZ	aTZ	aQZ
HCl						
$\omega(\sigma^+)$	3023	3044	3041	2971	2991	2989
$(HCl)_3$						
ω(e′)	2923	2920	2911	2899	2903	2899
ω(a′)	2889	2877	2868	2873	2871	2866
$\Delta\omega_{max}$	−134	−167	−174	−98	−120	−123
$(HCl)_4$						
ω(b)	2895	2889	2880	2883	2882	2877
ω(e)	2877	2867	2858	2869	2865	2861
ω(a)	2836	2818	2808	2839	2828	2824
$\Delta\omega_{max}$	−187	−226	−233	−133	−163	−166
$(HCl)_5$						
ω(a)	2891	2885	2878	2881	2880	—
ω(a)	2887	2880	2871	2878	2876	—
ω(a)	2863	2852	2843	2860	2855	—
ω(a)	2863	2851	2842	2860	2854	—
ω(a)	2830	2812	2803	2835	2825	—
$\Delta\omega_{max}$	−193	−232	−238	−136	−166	

Table 4 Imaginary harmonic vibrational frequencies (ω_i in cm^{-1} and labelled by irreducible representations) associated with the transition states for concerted proton transfer in $(HF)_n$, $(H_2O)_n$ and $(HCl)_n$, where n = 3, 4, 5

		MP2			CCSD(T)		
Cluster	Mode	aDZ	aTZ	aQZ	aDZ	aTZ	aQZ
$(HF)_3$	$\omega_i(a_2')$	1792i	1690i	1720i	1879i	1775i	1808i
$(HF)_4$	$\omega_i(a_{2g})$	1585i	1426i	1477i	1672i	1515i	1569i
$(HF)_5$	$\omega_i(a_2')$	1527i	1344i	1406i	1611i	1433i	1497i
$(H_2O)_3$	ω_i(a″)	1869i	1811i	1829i	1972i	1915i	1934i
$(H_2O)_4$	$\omega_i(a_2)$	1722i	1649i	1671i	1823i	1753i	1777i
$(H_2O)_5$	ω_i(a″)	1697i	1621i	1642i	1788i	1724i	—
$(HCl)_3$	$\omega_i(a_2')$	1486i	1496i	1475i	1627i	1652i	1635i
$(HCl)_4$	$\omega_i(a_2)$	1438i	1456i	1436i	1571i	1602i	1586i
$(HCl)_5$	ω_i(b)	1426i	1451i	1428i	1559i	1597i	—

3.3 Dissociation energies

The electronic dissociation energies (ΔE) near the MP2, CCSD and CCSD(T) CBS limits are reported in Table 5 for CCSD(T)/aQZ optimized structures of each cluster and corresponding monomer. With the exception of $(H_2O)_5$, the tabulated results are obtained using an average of 4 ΔE values: 2 from explicitly correlated computations with the ha5Z-F12 and a5Z-F12 basis sets along with 2 more from X = Q, 5, 6 CBS extrapolations using the ha$X$Z and aXZ families of basis sets. These 4 values (or 2 in the case of $(H_2O)_5$) tend to be very similar, typically deviating from the mean by a few hundredths of a kcal mol^{-1} and at most by ±0.13 kcal mol^{-1} for the HCl pentamer. For the case of $(H_2O)_5$, CCSD(T) computations were not feasible with the a6Z and ha6Z basis sets, and the ΔE values reported in Table 5 are merely the average of the a5Z-F12 and ha5Z-F12 explicitly correlated results. It is worth noting that these 3 average dissociation energies for the water pentamer do not change appreciably if the analogous X = T, Q, 5 extrapolations are included (by no more than 0.05 kcal mol^{-1} to give 36.34 ± 0.08, 33.86 ± 0.06 and 36.00 ± 0.06 kcal mol^{-1} for MP2, CCSD and CCSD(T), respectively).

Near the CBS limit, the CCSD(T) dissociation energies of $(HF)_3$ and $(H_2O)_3$ differ by only ≈0.5 kcal mol^{-1} (15.25 and 15.77 kcal mol^{-1}, respectively). The difference in ΔE is even smaller for the tetramers (27.71 kcal mol^{-1} for $(HF)_4$ and 27.45 kcal mol^{-1} for $(H_2O)_4$), whereas it grows to approximately 2 kcal mol^{-1} for the pentamers (38.08 kcal mol^{-1} for $(HF)_5$ *vs.* 36.05 kcal mol^{-1} for $(H_2O)_5$). This corresponds to at least 5.0, 6.8 and 7.2 kcal mol^{-1} per hydrogen bond for the homogeneous trimers, tetramers and pentamers of HF and H_2O based on the CCSD(T) ΔE values near the CBS limit. In contrast, the corresponding dissociation energies for the $(HCl)_n$ clusters range from approximately 2.2 to 2.7 kcal mol^{-1} per hydrogen bond (ΔE = 6.66, 10.37 and 13.28 kcal mol^{-1} for n = 3, 4, 5, respectively). The CCSD(T) CBS ΔE values from this work are typically within a few tenths of a kcal mol^{-1} of other benchmark

Table 5 Estimates of the MP2, CCSD and CCSD(T) electronic dissociation energies (ΔE in kcal mol^{-1}) at the CBS limit for the CCSD(T)/aQZ optimized structures obtained from the average of two explicitly correlated values computed with the a5Z-F12 and ha5Z-F12 basis sets and two extrapolated values[a] from the aXZ and ha$X$Z series of basis sets with X = Q, 5, 6, where the ± data denote the range of these values about the mean (not error bars)

Cluster	MP2	CCSD	CCSD(T)	Other	CCSD(T)
$(HF)_3$	14.94 ± 0.01	14.33 ± 0.02	15.26 ± 0.03	15.3[b]	15.1[c]
$(HF)_4$	27.66 ± 0.04	26.26 ± 0.02	27.91 ± 0.03	27.7[b]	27.4[c]
$(HF)_5$	37.90 ± 0.05	35.97 ± 0.03	38.08 ± 0.04	37.8[b]	37.4[c]
$(H_2O)_3$	15.81 ± 0.02	14.77 ± 0.01	15.77 ± 0.01	15.8[d]	15.8[e]
$(H_2O)_4$	27.66 ± 0.04	25.77 ± 0.01	27.46 ± 0.02	27.4[e]	27.8[f]
$(H_2O)_5$[a]	36.32 ± <0.01	33.91 ± <0.01	36.05 ± <0.01	35.9[e]	36.4[f]
$(HCl)_3$	7.63 ± 0.03	5.51 ± 0.06	6.66 ± 0.06	6.8[g]	
$(HCl)_4$	11.94 ± 0.05	8.60 ± 0.09	10.37 ± 0.10	—	
$(HCl)_5$	15.33 ± 0.06	10.97 ± 0.12	13.28 ± 0.13	—	

[a] Average of a5Z-F12 and ha5Z-F12 for $(H_2O)_5$. [b] Ref. 35. [c] Ref. 136. [d] Ref. 92. [e] Ref. 137. [f] Ref. 138. [g] Ref. 73.

CCSD(T) results for these systems,[35,73,92,136–138] such as those listed in the last column of Table 5.

The estimates of the MP2 ΔE values at the CBS limit in Table 5 are within 0.3 kcal mol^{-1} of the CCSD(T) results for the $(HF)_n$ and $(H_2O)_n$ clusters, but MP2 tends to overestimate the CCSD(T) results by 1 or 2 kcal mol^{-1} for the $(HCl)_n$ systems. In contrast, the CCSD CBS limit dissociation energies in Table 5 are always smaller than the CCSD(T) values by roughly 1–2 kcal mol^{-1}.

Although correlation consistent basis sets with an additional set of tight d-functions (aug-cc-pV(X+d)Z) are available for Cl,[139] we found that replacing the ha$X$Z and aXZ basis sets with their ha(X+d)Z and a(X+d)Z counterparts changed the CBS values reported for $(HCl)_3$ and $(HCl)_4$ in Table 5 by no more than 0.01 kcal mol^{-1}, while the corresponding ranges changed by no more than ±0.01 kcal mol^{-1} for the trimer and ±0.03 kcal mol^{-1} for the tetramer. These observations are consistent with our previous findings regarding the negligible impact of tight d-functions on non-covalent dimers containing HCl or H_2S.[113,140–143] The ΔE values obtained from each level of theory and from the extrapolations can be found in Tables S37–S45 of the ESI.†

3.4 Barrier heights

The same procedures were used to estimate the electronic barrier heights (ΔE^*) for CPT in each cluster near the CBS limit for the MP2, CCSD and CCSD(T) methods. These results are reported in Table 6 for the CCSD(T)/aQZ optimized structures of each minimum and TS structure. As with ΔE, the ΔE^* results from X = Q, 5, 6 extrapolations are quite similar to those from the ha5Z-F12 and a5Z-F12 explicitly correlated computations, all 4 values typically falling within a few hundredths of a kcal mol^{-1} of the mean and never deviating from it by more than ±0.14 kcal mol^{-1} for $(HCl)_5$.

$(HF)_4$ and $(HF)_5$ have the smallest barriers for CPT, by far. Both values are nearly identical and less than 15 kcal mol^{-1} at the CCSD(T) CBS limit (14.8 and 14.9 kcal mol^{-1}, respectively). $(HF)_3$ has the closest barrier height to these values, but ΔE^* increases by more than 5 kcal mol^{-1} (to 20.7 kcal mol^{-1}). All of the other electronic barriers for CPT for these clusters are at least another 6 kcal mol^{-1} larger at the CCSD(T) CBS limit,

Table 6 Estimates of the MP2, CCSD and CCSD(T) electronic CPT barrier heights (ΔE^* in kcal mol^{-1}) at the CBS limit for the CCSD(T)/aQZ optimized structures obtained from the average of two explicitly correlated values computed with the a5Z-F12 and ha5Z-F12 basis sets and two extrapolated values[a] from the aXZ and ha$X$Z series of basis sets with X = Q, 5, 6, where the ± data denote the range of these values about the mean (not error bars)

Cluster	MP2	CCSD	CCSD(T)	Other CCSD(T)
$(HF)_3$	18.87 ± 0.04	23.31 ± 0.01	20.67 ± 0.03	20.3[b]
$(HF)_4$	12.99 ± 0.04	17.35 ± 0.02	14.81 ± 0.02	14.3[b]
$(HF)_5$	12.85 ± 0.05	17.61 ± 0.03	14.87 ± 0.03	15.5[b]
$(H_2O)_3$	27.09 ± 0.02	33.24 ± 0.01	29.99 ± 0.01	—
$(H_2O)_4$	23.62 ± 0.01	30.43 ± 0.02	26.90 ± 0.01	—
$(H_2O)_5$[a]	26.61 ± <0.01	34.56 ± <0.01	30.43 ± <0.01	—
$(HCl)_3$	22.51 ± 0.04	32.50 ± 0.08	27.43 ± 0.06	—
$(HCl)_4$	24.95 ± 0.03	37.09 ± 0.11	30.98 ± 0.08	—
$(HCl)_5$	30.50 ± 0.04	45.55 ± 0.14	38.04 ± 0.11	—

[a] Average of a5Z-F12 and ha5Z-F12 for $(H_2O)_5$. [b] Ref. 35.

where ΔE^* is around 27 kcal mol^{-1} for both $(H_2O)_4$ and $(HCl)_3$ (26.9 and 27.4 kcal mol^{-1}, respectively). These barriers grow by approximately another 3–4 kcal mol^{-1} for $(H_2O)_3$ (30.0 kcal mol^{-1}), $(H_2O)_5$ (30.4 kcal mol^{-1}) and $(HCl)_4$ (31.0 kcal mol^{-1}). Lastly, ΔE^* jumps to 38.0 kcal mol^{-1} at the CCSD(T) CBS limit for the HCl pentamer.

Prior estimates of CCSD(T) barrier heights for CPT in these systems are available for $(HF)_{n=3,4,5}$ and summarized in Table 6 of ref. 35. Our CCSD(T) CBS ΔE^* values in Table 6 are within ≈1 kcal mol^{-1} of the final barrier heights reported in that study (85, 60 and 65 kJ mol^{-1} for $(HF)_{n=3,4,5}$, respectively, with conservative uncertainties of ±10 kJ mol^{-1}).

We are not aware of any CCSD(T) barrier heights that have been reported in previous studies for the $(H_2O)_n$ clusters examined here. However, an early study reported MP4 ΔE^* values computed with a double-ζ basis set for $(H_2O)_3$ and $(H_2O)_4$ (28.8 and 25.0 kcal mol^{-1}, respectively) that are only about 1 kcal mol^{-1} smaller than our current estimates at the CCSD(T) CBS limit.[76] In addition, a number of MP2 barrier heights for CPT have been reported for these small cyclic water clusters,[33,77,79] and the values are typically within *ca.* 1 kcal mol^{-1} of the MP2 CBS limits tabulated in the first column of data in Table 6.

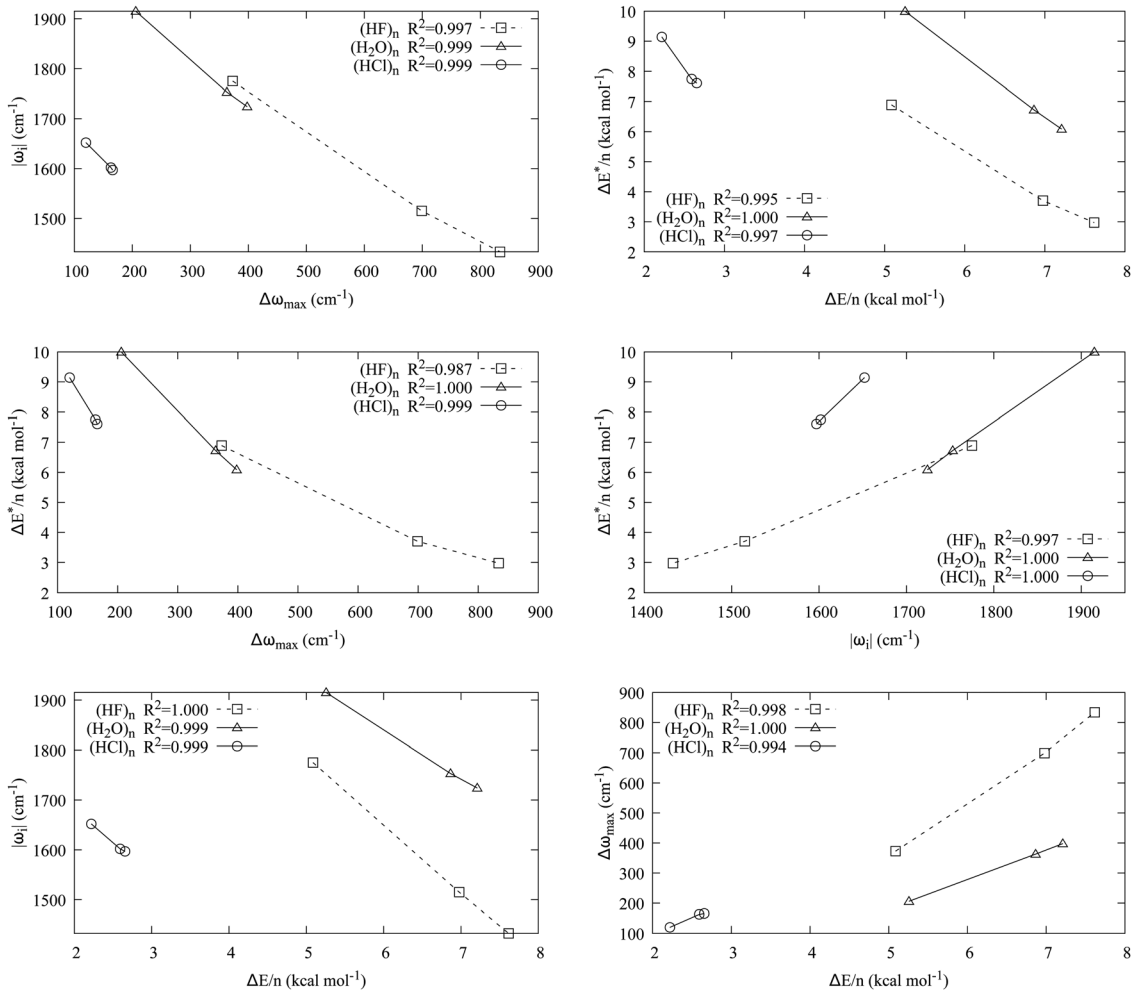

Fig. 5 Examples of linear relationships within each cluster family involving properties of the TS (magnitude of the imaginary vibrational frequency ($|\omega_i|$) and barrier height per fragment ($\Delta E^*/n$)) and/or properties of the minimum (maximum vibrational frequency shift relative to the monomer ($\Delta\omega_{max}$) and dissociation energy per fragment ($\Delta E/n$)).

One investigation computed barrier heights for CPT in $(HCl)_3$ with a variety of methods including MP2, MP4 and QCISD(T) utilizing triple-ζ split-valence basis sets.[31] Those barrier heights ranged from approximately 25 to 32 kcal mol^{-1}, which are reasonably similar to the MP2, CCSD and CCSD(T) CBS values reported in Table 6 for the HCl trimer. We are not aware of any studies that have reported ΔE^* for $(HCl)_4$ or $(HCl)_5$.

The MP2 CBS barrier heights in Table 6 are always smaller than the corresponding CCSD(T) CBS values by *ca.* 2 kcal mol^{-1} for the $(HF)_n$ clusters, by *ca.* 3 kcal mol^{-1} for the $(H_2O)_n$ clusters and by 5 kcal mol^{-1} or more for the $(HCl)_n$ clusters. In contrast, the CCSD method overestimates the CCSD(T) ΔE^* values at the CBS limit, typically by a slightly larger magnitude. Additional computations were carried out on the TS structures of $(HCl)_3$ and $(HCl)_4$ with the correlation consistent basis sets that include an additional set of tight d-functions. As with ΔE (previous section), the effect on ΔE^* was negligible. The CBS values reported in Table 6 changed by no more than 0.01 kcal mol^{-1} and the corresponding ranges changed by no more than $\pm$0.03 kcal mol^{-1}. The ΔE^* values obtained from each level of theory and from the extrapolations can be found in Tables S37–S45 of the ESI.†

4 Conclusions

For the homogeneous trimers examined in this study, $(HF)_3$ and $(H_2O)_3$ have very similar electronic dissociation energies at the CCSD(T) CBS limit (ΔE = 15.26 and 15.77 kcal mol^{-1}, respectively), whereas the corresponding value for $(HCl)_3$ is smaller by more than a factor of two (ΔE = 6.66 kcal mol^{-1}). The CCSD(T) CBS limit electronic barrier heights for CPT in these systems (ΔE^*) follow a different trend, increasing from 20.67 kcal mol^{-1} for $(HF)_3$ to 27.43 kcal mol^{-1} for $(HCl)_3$ and finally 29.99 kcal mol^{-1} for $(H_2O)_3$.

The tetramers exhibit the same trend in ΔE, with similar values at the CCSD(T) CBS limit for $(HF)_4$ and $(H_2O)_4$ (27.91 and 27.46 kcal mol^{-1}, respectively) but significantly smaller for $(HCl)_4$ (10.37 kcal mol^{-1}). A different pattern is observed for

the CPT barriers. $(HF)_4$ has the smallest ΔE^* out of the 9 clusters examined in this study (only 14.81 kcal mol^{-1} at the CCSD(T) CBS limit). The barrier height nearly doubles in the water tetramer (26.90 kcal mol^{-1}) and more than doubles in the HCl tetramer (30.98 kcal mol^{-1}).

For n = 5, the HF and H_2O clusters again have much larger dissociation energies at the CCSD(T) CBS limit than the HCl system (38.08 kcal mol^{-1} for $(HF)_5$ and 36.05 kcal mol^{-1} for $(H_2O)_5$ *vs.* 13.28 kcal mol^{-1} for $(HCl)_5$). Interestingly, ΔE for $(HF)_5$ is 2 kcal mol^{-1} larger than $(H_2O)_5$ even though $(HF)_n$ and $(H_2O)_n$ had very similar dissociation energies for n = 3 and 4. These pentamers follow the same trend in CCSD(T) CBS barrier heights as the tetramers, with ΔE^* increasing dramatically from only 14.87 kcal mol^{-1} for $(HF)_5$ to 30.43 kcal mol^{-1} for $(H_2O)_5$ and 38.04 kcal mol^{-1} for $(HCl)_5$.

Overall, these well-converged estimates of the CCSD(T) CBS limit will help anchor the electronic barrier heights for CPT in a number of these important cyclic hydrogen-bonded clusters for which prior ΔE^* values were not available or had very large uncertainties. For example, previous *ab initio* estimates of ΔE^* for the HCl trimer computed with various triple-ζ basis sets ranged from roughly 25 to 32 kcal mol^{-1} for the HCl trimer[31] and from approximately 25 to 29 kcal mol^{-1} for the H_2O trimer.[77–79] This work conclusively demonstrates not only that ΔE^* for the HCl trimer is appreciably smaller than for the H_2O trimer (by $\approx$2.5 kcal mol^{-1} near the CCSD(T) CBS limit) but also that the situation reverses for the tetramers and pentamers where the CCSD(T) CBS ΔE^* is significantly larger for $(HCl)_n$ than $(H_2O)_n$ (by more than 4 and 7 kcal mol^{-1} for n = 4 and 5, respectively). In addition, these are the first barrier heights reported for CPT in $(HCl)_4$ and $(HCl)_5$, to the best of our knowledge. Similar estimates for the electronic barrier height in $(H_2O)_4$ ranged from *ca.* 23 to 29 kcal mol^{-1}.[77,79] The CCSD(T) CBS estimates presented here indicate that the H_2O tetramer has a barrier height around 27 kcal mol^{-1} (more than 3 kcal mol^{-1} smaller than the trimer and pentamer), which suggests that surface effects could substantially lower the electronic barrier in this system (to $<$20 kcal mol^{-1}) as indicated by the density functional theory (DFT) computations carried out in ref. 27 to corroborate their experimental observation of CPT in $(H_2O)_4$.

Within each family of homogeneous cyclic hydrogen bonded trimers, tetramers and pentamers, some interesting relationships emerge between the various vibrational and energetic quantities tabulated in the previous section. For example, the top left panel of Fig. 5 shows strong linear relationships between the magnitude of imaginary vibrational frequency of the TS ($|\omega_i|$) and the maximum vibrational frequency shift of the mimimum relative to the monomer ($\Delta\omega_{max}$). The R^2 value is 0.997 for the $(HF)_n$ data, and it increases to 0.999 for both the $(H_2O)_n$ and $(HCl)_n$ series. Scaling both the dissociation energies and barrier heights by the number of fragments ($\Delta E/n$ and $\Delta E^*/n$, respectively) also reveals a strong linear correlation ($R^2 \geq 0.995$) between the two quantities for each cluster family (top right panel of Fig. 5). In addition, the barrier height per fragment has good linear relationships ($R^2 \geq 0.987$) with both $|\omega_i|$ and $\Delta\omega_{max}$ as shown in the middle two panels of Fig. 5. These two vibrational frequency quantities exhibit good linear correlations with the dissociation energy per fragment ($\Delta E/n$) as well (bottom two panels of Fig. 5).

Although it is tempting to infer broad generalizations from these trends, any conclusions drawn from the strong correlations reported here should be tempered by the limited sample size, only 3 data points in each $(HF)_n$, $(H_2O)_n$ and $(HCl)_n$ series. We are in the process of expanding this analysis to more diverse sets of hydrogen bonded clusters (*e.g.*, heterogeneous clusters and other fragments). Additionally, the CCSD(T) energetics determined near the CBS limit and CCSD(T) harmonic vibrational frequencies computed with the aTZ and aQZ basis sets are being used to calibrate less demanding procedures that can be reliably used to examine related systems and larger clusters.

Conflicts of interest

There are no conflicts to declare.

Acknowledgements

The authors acknowledge the Mississippi Center for Supercomputing Research for access to their computational resources. This work was funded in part by the National Science Foundation (CHE-2154403).

References

1 *Proton Transfer in Hydrogen-bonded Systems*, ed. T. Bountis, NATO ASI series B: Physics, Plenum, New York, 1st edn, 1992, vol. 291.
2 *Hydrogen-Transfer Reactions*, ed. J. T. Hynes, J. P. Klinman, H.-H. Limbach and R. L. Schowen, Verlag GmbH & Co. KGaA, Weinheim, Germany, 2007, vol. 1–4.
3 T. Matsui, Y. Shigeta and K. Hirao, *J. Phys. Chem. B*, 2007, **111**, 1176–1181.
4 D. Jacquemin, J. Zúñiga, A. Requena and J. P. Céron-Carrasco, *Acc. Chem. Res.*, 2014, **47**, 2467–2474.
5 J. Meisner and J. Kästner, *Angew. Chem., Int. Ed.*, 2016, **55**, 5400–5413.
6 R. Srivastava, *Front. Chem.*, 2019, **7**, 546.
7 J. M. Mayer and I. J. Rhile, *Biochim. Biophys. Acta, Bioenerg.*, 2004, **1655**, 51–58.
8 S. Schweiger, B. Hartke and G. Rauhut, *Phys. Chem. Chem. Phys.*, 2005, **7**, 493–500.
9 Z. Smedarchina, W. Siebrand and A. Fernández-Ramos, *Hydrogen-Transfer Reactions*, Verlag GmbH & Co. KGaA, Weinheim, Germany, 2007, ch. 29, vol. 2, pp. 895–945.
10 Z. Smedarchina, W. Siebrand, A. Fernández-Ramos and R. Meana-Pañeda, *Z. Phys. Chem.*, 2008, **222**, 1291–1309.
11 Z. Smedarchina, W. Siebrand and A. Fernández-Ramos, *J. Phys. Chem. A*, 2013, **117**, 11086–11100.
12 Y.-H. Cheng, Y.-C. Zhu, X.-Z. Li and W. Fang, *Chin. Phys. B*, 2023, **32**, 018201.

13 T. Loerting and K. R. Liedl, *J. Am. Chem. Soc.*, 1998, **120**, 12595–12600.
14 Y. Podolyan, L. Gorb and J. Leszczynski, *J. Phys. Chem. A*, 2002, **106**, 12103–12109.
15 M. Meuwly, A. Müller and S. Leutwyler, *Phys. Chem. Chem. Phys.*, 2003, **5**, 2663–2672.
16 P. Zielke and M. A. Suhm, *Phys. Chem. Chem. Phys.*, 2007, **9**, 4528–4534.
17 Ö. Birer and M. Havenith, *Ann. Rev. Phys. Chem.*, 2009, **60**, 263–275.
18 G. Feng, L. B. Favero, A. Maris, A. Vigorito, W. Caminati and R. Meyer, *J. Am. Chem. Soc.*, 2012, **134**, 19281–19286.
19 C. Qu and J. M. Bowman, *Faraday Discuss.*, 2018, **212**, 33–49.
20 D. Kurzydłowski, *RSC Adv.*, 2022, **12**, 11436–11441.
21 A. Baldy, J. Elguero, R. Faure, M. Pierrot and E. J. Vincent, *J. Am. Chem. Soc.*, 1985, **107**, 5290–5291.
22 J. A. S. Smith, B. Wehrle, F. Aguilar-Parrilla, H. H. Limbach, M. D. L. C. Foces-Foces, F. Hernández Cano, J. Elguero, A. Baldy, M. Pierrot, M. M. T. Khurshid and J. B. Larcombe-McDouall, *J. Am. Chem. Soc.*, 1989, **111**, 7304–7312.
23 F. Aguilar-Parrilla, G. Scherer, H. H. Limbach, M. D. L. C. Foces-Foces, F. Hernandez Cano, J. A. S. Smith, C. Toiron and J. Elguero, *J. Am. Chem. Soc.*, 1992, **114**, 9657–9659.
24 D. F. Brougham, R. Caciuffo and A. J. Horsewill, *Nature*, 1999, **397**, 241–243.
25 O. Klein, F. Aguilar-Parrilla, J. M. Lopez, N. Jagerovic, J. Elguero and H.-H. Limbach, *J. Am. Chem. Soc.*, 2004, **126**, 11718–11732.
26 L. E. Bove, S. Klotz, A. Paciaroni and F. Sacchetti, *Phys. Rev. Lett.*, 2009, **103**, 165901.
27 X. Meng, J. Guo, J. Peng, J. Chen, Z. Wang, J.-R. Shi, X.-Z. Li, E.-G. Wang and Y. Jiang, *Nat. Phys.*, 2015, **11**, 235–239.
28 J. F. Gaw, Y. Yamaguchi, M. A. Vincent and H. F. I. Schaefer, *J. Am. Chem. Soc.*, 1984, **106**, 3133–3138.
29 A. Karpfen, *Int. J. Quantum Chem.*, 1990, **38**, 129–140.
30 A. Komornicki, D. A. Dixon and P. R. Taylor, *J. Chem. Phys.*, 1992, **96**, 2920–2925.
31 D. Heidrich, N. J. R. van Eikema Hommes and P. von Ragué Schleyer, *J. Comput. Chem.*, 1993, **14**, 1149–1163.
32 K. R. Liedl, R. T. Kroemer and B. M. Rode, *Chem. Phys. Lett.*, 1995, **246**, 455–462.
33 K. R. Liedl, S. Sekusak, R. T. Kroemer and B. M. Rode, *J. Phys. Chem. A*, 1997, **101**, 4707–4716.
34 C. Maerker, P. V. R. Schleyer, K. Liedl, T.-K. Ha, M. Quack and M. A. Suhm, *J. Comput. Chem.*, 1997, **18**, 1695–1719.
35 W. Klopper, M. Quack and M. A. Suhm, *Mol. Phys.*, 1998, **94**, 105–116.
36 T. Loerting, K. R. Liedl and B. M. Rode, *J. Am. Chem. Soc.*, 1998, **120**, 404–412.
37 T. Loerting and K. R. Liedl, *J. Phys. Chem. A*, 1999, **103**, 9022–9028.
38 T. A. Blake, S. W. Sharpe and S. S. Xantheas, *J. Chem. Phys.*, 2000, **113**, 707–718.
39 M. Kreitmeir, G. Heusel, H. Bertagnolli, K. Tödheide, C. J. Mundy and G. J. Cuello, *J. Chem. Phys.*, 2005, **122**, 154511.
40 S. F. de, A. Morais, K. C. Mundim and D. A. C. Ferreira, *Theor. Chem. Acc.*, 2020, **139**, 164.
41 J. M. Lisy, A. Tramer, M. F. Vernon and Y. T. Lee, *J. Chem. Phys.*, 1981, **75**, 4733–4734.
42 D. W. Michael and J. M. Lisy, *J. Chem. Phys.*, 1986, **85**, 2528–2537.
43 K. D. Kolenbrander, C. E. Dykstra and J. M. Lisy, *J. Chem. Phys.*, 1988, **88**, 5995–6012.
44 G. Chałasiński, S. M. Cybulski, M. M. Szczęśniak and S. Scheiner, *J. Chem. Phys.*, 1989, **91**, 7048–7056.
45 M. Quack, U. Schmitt and M. A. Suhm, *Chem. Phys. Lett.*, 1993, **208**, 446–452.
46 M. Quack, J. Stohner and M. A. Suhm, *J. Mol. Struct.*, 1993, **294**, 33–36.
47 M. A. Suhm, J. Farrell, T. John, S. H. Ashworth and D. J. Nesbitt, *J. Chem. Phys.*, 1993, **98**, 5985–5989.
48 A. Karpfen and O. Yanovitskii, *THEOCHEM*, 1994, **307**, 81–97.
49 A. Karpfen and O. Yanovitskii, *THEOCHEM*, 1994, **314**, 211–227.
50 F. Huisken, M. Kaloudis, A. Kulcke, C. Laush and J. M. Lisy, *J. Chem. Phys.*, 1995, **103**, 5366–5377.
51 F. Huisken, E. G. Tarakanova, A. A. Vigasin and G. V. Yukhnevich, *Chem. Phys. Lett.*, 1995, **245**, 319–325.
52 D. Luckhaus, M. Quack, U. Schmitt and M. A. Suhm, *Ber. Bunsenges. Phys. Chem.*, 1995, **99**, 457–468.
53 M. A. Suhm, *Ber. Bunsenges. Phys. Chem.*, 1995, **99**, 1159–1167.
54 G. S. Tschumper, Y. Yamaguchi and H. F. Schaefer, *J. Chem. Phys.*, 1997, **106**, 9627–9633.
55 M. Quack and M. A. Suhm, *Conceptual Perspectives in Quantum Chemistry*, Kluwer Pub. Co., Dordrecht, 1997, vol. III, pp. 415–464.
56 M. Quack and M. A. Suhm, *Adv. Mol. Vibrations Collision Dynamics*, 1998, **3**, 205–248.
57 L. Oudejans and R. E. Miller, *J. Chem. Phys.*, 2000, **113**, 971–978.
58 M. Quack, J. Stohner and M. A. Suhm, *J. Mol. Struct.*, 2001, **599**, 381–425.
59 G. E. Douberly and R. E. Miller, *J. Phys. Chem. B*, 2003, **107**, 4500–4507.
60 G. S. Tschumper, *Chem. Phys. Lett.*, 2006, **427**, 185–191.
61 M. J. McGrath, J. N. Ghogomu, C. J. Mundy, I.-F. W. Kuo and J. I. Siepmann, *Phys. Chem. Chem. Phys.*, 2010, **12**, 7678–7687.
62 P. Asselin, P. Soulard, B. Madebène, M. Goubet, T. R. Huet, R. Georges, O. Pirali and P. Roy, *Phys. Chem. Chem. Phys.*, 2014, **16**, 4797–4806.
63 D. K. Hindermann and C. D. Cornwell, *J. Chem. Phys.*, 1968, **48**, 2017–2025.
64 K. von Puttkamer and M. Quack, *Chem. Phys.*, 1989, **139**, 31–53.
65 J. Han, Z. Wang, A. L. McIntosh, R. R. Lucchese and J. W. Bevan, *J. Chem. Phys.*, 1994, **100**, 7101–7108.

66 W. D. Chandler, K. E. Johnson, B. D. Fahlman and J. L. E. Campbell, *Inorg. Chem.*, 1997, **36**, 776–781.
67 Z. Latajka and S. Scheiner, *Chem. Phys.*, 1997, **216**, 37–52.
68 T. Häber, U. Schmitt and M. A. Suhm, *Phys. Chem. Chem. Phys.*, 1999, **1**, 5573–5582.
69 M. Fárník, S. Davis and D. J. Nesbitt, *Faraday Discuss.*, 2001, **118**, 63–78.
70 R. C. Guedes, P. C. do Couto and B. J. Costa Cabral, *J. Chem. Phys.*, 2003, **118**, 1272–1281.
71 D. Skvortsov, M. Y. Choi and A. F. Vilesov, *J. Phys. Chem. A*, 2007, **111**, 12711–12716.
72 M. W. Avilés, M. L. McCandless and E. Curotto, *J. Chem. Phys.*, 2008, **128**, 124517.
73 J. S. Mancini and J. M. Bowman, *J. Phys. Chem. A*, 2014, **118**, 7367–7374.
74 J. S. Mancini, A. K. Samanta, J. M. Bowman and H. Reisler, *J. Phys. Chem. A*, 2014, **118**, 8402–8410.
75 A. K. Samanta, Y. Wang, J. S. Mancini, J. M. Bowman and H. Reisler, *Chem. Rev.*, 2016, **116**, 4913–4937.
76 B. C. Garrett and C. F. Melius, *Theoretical and Computational Models for Organic Chemistry*, NATO ASI Series, Springer, Dordrecht, 1991, vol. 339, pp. 35–54.
77 T. Loerting, K. R. Liedl and B. M. Rode, *J. Chem. Phys.*, 1998, **109**, 2672–2679.
78 Z. Smedarchina, A. Fernández-Ramos and W. Siebrand, *J. Comput. Chem.*, 2001, **22**, 787–801.
79 Y. Kim and Y. Kim, *J. Phys. Chem. A*, 2006, **110**, 600–608.
80 H. Cybulski and J. Sadlej, *J. Phys. Chem. A*, 2011, **115**, 5774–5784.
81 N. Pugliano and R. Saykally, *Science*, 1992, **257**, 1937–1940.
82 K. Liu, M. G. Brown, J. D. Cruzan and R. J. Saykally, *Science*, 1996, **271**, 62–64.
83 J. D. Cruzan, L. B. Braly, K. Liu, M. G. Brown, J. G. Loeser and R. J. Saykally, *Science*, 1996, **271**, 59–62.
84 D. J. Wales and T. R. Walsh, *J. Chem. Phys.*, 1996, **105**, 6957–6971.
85 T. R. Walsh and D. J. Wales, *J. Chem. Soc., Faraday Trans.*, 1996, **92**, 2505–2517.
86 D. J. Wales and T. R. Walsh, *J. Chem. Phys.*, 1997, **106**, 7193–7207.
87 K. Liu, M. G. Brown, J. D. Cruzan and R. J. Saykally, *J. Phys. Chem. A*, 1997, **101**, 9011–9021.
88 K. Liu, M. G. Brown and R. J. Saykally, *J. Phys. Chem. A*, 1997, **101**, 8995–9010.
89 J. D. Cruzan, M. R. Viant, M. G. Brown and R. J. Saykally, *J. Phys. Chem. A*, 1997, **101**, 9022–9031.
90 F. N. Keutsch and R. J. Saykally, *Proc. Natl. Acad. Sci. U. S. A.*, 2001, **98**, 10533–10540.
91 F. N. Keutsch, J. D. Cruzan and R. J. Saykally, *Chem. Rev.*, 2003, **103**, 2533–2578.
92 J. A. Anderson, K. Crager, L. Fedoroff and G. S. Tschumper, *J. Chem. Phys.*, 2004, **121**, 11023–11029.
93 M. Takahashi, Y. Watanabe, T. Taketsugu and D. J. Wales, *J. Chem. Phys.*, 2005, **123**, 044302.
94 H. A. Harker, M. R. Viant, F. N. Keutsch, E. A. Michael, R. P. McLaughlin and R. J. Saykally, *J. Phys. Chem. A*, 2005, **109**, 6483–6497.
95 J. Han, L. K. Takahashi, W. Lin, E. Lee, F. N. Keutsch and R. J. Saykally, *Chem. Phys. Lett.*, 2006, **423**, 344–351.
96 W. Lin, J.-X. Han, L. K. Takahashi, H. A. Harker, F. N. Keutsch and R. J. Saykally, *J. Chem. Phys.*, 2008, **128**, 094302.
97 W. T. S. Cole, R. S. Fellers, M. R. Viant and R. J. Saykally, *J. Chem. Phys.*, 2017, **146**, 014306.
98 M. T. Cvitaš and J. O. Richardson, *Molecular Spectroscopy and Quantum Dynamics*, Elsevier, St. Louis, Missouri, 2021, ch. 9, pp. 301–326.
99 M. Mandziuk, *Chem. Phys. Lett.*, 2016, **661**, 263–268.
100 M. Mandziuk, *J. Mol. Struct.*, 2019, **1177**, 168–176.
101 L. De Marco, J. A. Fournier, M. Thämer, W. Carpenter and A. Tokmakoff, *J. Chem. Phys.*, 2016, **145**, 094501.
102 C. Møller and M. S. Plesset, *Phys. Rev.*, 1934, **46**, 618–622.
103 J. Čížek, *J. Chem. Phys.*, 1966, **45**, 4256–4266.
104 G. D. Purvis and R. J. Bartlett, *J. Chem. Phys.*, 1982, **76**, 1910–1918.
105 K. Raghavachari, G. W. Trucks, J. A. Pople and M. Head-Gordon, *Chem. Phys. Lett.*, 1989, **157**, 479–483.
106 T. H. Dunning, *J. Chem. Phys.*, 1989, **90**, 1007–1023.
107 R. A. Kendall, T. H. Dunning and R. J. Harrison, *J. Chem. Phys.*, 1992, **96**, 6796–6806.
108 D. E. Woon and T. H. Dunning, *J. Chem. Phys.*, 1993, **98**, 1358–1371.
109 N. R. Kestner, *J. Chem. Phys.*, 1968, **48**, 252–257.
110 B. Liu and A. D. McLean, *J. Chem. Phys.*, 1973, **59**, 4557–4558.
111 H. B. Jansen and P. Ros, *Chem. Phys. Lett.*, 1969, **3**, 140–143.
112 S. F. Boys and F. Bernardi, *Mol. Phys.*, 1970, **19**, 553.
113 M. A. Perkins, K. R. Barlow, K. M. Dreux and G. S. Tschumper, *J. Chem. Phys.*, 2020, **152**, 214306.
114 D. Feller, *J. Chem. Phys.*, 1993, **98**, 7059–7071.
115 T. Helgaker, W. Klopper, H. Koch and J. Noga, *J. Chem. Phys.*, 1997, **106**, 9639–9646.
116 T. B. Adler, G. Knizia and H.-J. Werner, *J. Chem. Phys.*, 2007, **127**, 221106.
117 G. Knizia, T. B. Adler and H.-J. Werner, *J. Chem. Phys.*, 2009, **130**, 054104.
118 C. Hättig, D. P. Tew and A. Köhn, *J. Chem. Phys.*, 2010, **132**, 231102.
119 H.-J. Werner, G. Knizia and F. R. Manby, *Mol. Phys.*, 2011, **109**, 407–417.
120 K. A. Peterson, T. B. Adler and H.-J. Werner, *J. Chem. Phys.*, 2008, **128**, 084102.
121 N. Sylvetsky, M. K. Kesharwani and J. M. L. Martin, *J. Chem. Phys.*, 2017, **147**, 134106.
122 H.-J. Werner, P. J. Knowles, P. Celani, W. Györffy, A. Hesselmann, D. Kats, G. Knizia, A. Köhn, T. Korona, D. Kreplin, R. Lindh, Q. Ma, F. R. Manby, A. Mitrushenkov, G. Rauhut, M. Schütz, K. R. Shamasundar, T. B. Adler, R. D. Amos, S. J. Bennie, A. Bernhardsson, A. Berning,

J. A. Black, P. J. Bygrave, R. Cimiraglia, D. L. Cooper, D. Coughtrie, M. J. O. Deegan, A. J. Dobbyn, K. Doll, M. Dornbach, F. Eckert, S. Erfort, E. Goll, C. Hampel, G. Hetzer, J. G. Hill, M. Hodges, T. Hrenar, G. Jansen, C. Köppl, C. Kollmar, S. J. R. Lee, Y. Liu, A. W. Lloyd, R. A. Mata, A. J. May, B. Mussard, S. J. McNicholas, W. Meyer, T. F. Miller III, M. E. Mura, A. Nicklass, D. P. O'Neill, P. Palmieri, D. Peng, K. A. Peterson, K. Pflüger, R. Pitzer, I. Polyak, M. Reiher, J. O. Richardson, J. B. Robinson, B. Schröder, M. Schwilk, T. Shiozaki, M. Sibaev, H. Stoll, A. J. Stone, R. Tarroni, T. Thorsteinsson, J. Toulouse, M. Wang, M. Welborn and B. Ziegler, *MOLPRO, version 2022.1, a package of ab initio programs*, see **https://www.molpro.net**.

123 H.-J. Werner, P. Knowles, G. Knizia, F. Manby and M. Schütz, *Wiley Interdiscip. Rev.: Comput. Mol. Sci.*, 2012, **2**, 242–253.

124 H.-J. Werner, P. J. Knowles, F. R. Manby, J. A. Black, K. Doll, A. Heßelmann, D. Kats, A. Köhn, T. Korona, D. A. Kreplin, Q. Ma, I. Miller, F. Thomas, A. Mitrushchenkov, K. A. Peterson, I. Polyak, G. Rauhut and M. Sibaev, *J. Chem. Phys.*, 2020, **152**, 144107.

125 M. J. Frisch, G. W. Trucks, H. B. Schlegel, G. E. Scuseria, M. A. Robb, J. R. Cheeseman, G. Scalmani, V. Barone, G. A. Petersson, H. Nakatsuji, X. Li, M. Caricato, A. V. Marenich, J. Bloino, B. G. Janesko, R. Gomperts, B. Mennucci, H. P. Hratchian, J. V. Ortiz, A. F. Izmaylov, J. L. Sonnenberg, D. Williams-Young, F. Ding, F. Lipparini, F. Egidi, J. Goings, B. Peng, A. Petrone, T. Henderson, D. Ranasinghe, V. G. Zakrzewski, J. Gao, N. Rega, G. Zheng, W. Liang, M. Hada, M. Ehara, K. Toyota, R. Fukuda, J. Hasegawa, M. Ishida, T. Nakajima, Y. Honda, O. Kitao, H. Nakai, T. Vreven, K. Throssell, J. A. Montgomery, Jr., J. E. Peralta, F. Ogliaro, M. J. Bearpark, J. J. Heyd, E. N. Brothers, K. N. Kudin, V. N. Staroverov, T. A. Keith, R. Kobayashi, J. Normand, K. Raghavachari, A. P. Rendell, J. C. Burant, S. S. Iyengar, J. Tomasi, M. Cossi, J. M. Millam, M. Klene, C. Adamo, R. Cammi, J. W. Ochterski, R. L. Martin, K. Morokuma, O. Farkas, J. B. Foresman and D. J. Fox, *Gaussian16 Revision C.01*, Gaussian Inc., Wallingford CT, 2016.

126 J. F. Stanton, J. Gauss, L. Cheng, M. E. Harding, D. A. Matthews and P. G. Szalay, CFOUR version 2.1, Coupled-Cluster techniques for Computational Chemistry, a quantum-chemical program package, With contributions from A. A. Auer, R. J. Bartlett, U. Benedikt, C. Berger, D. E. Bernholdt, S. Blaschke, Y. J. Bomble, S. Burger, O. Christiansen, D. Datta, F. Engel, R. Faber, J. Greiner, M. Heckert, O. Heun, M. Hilgenberg, C. Huber, T.-C. Jagau, D. Jonsson, J. Jusélius, T. Kirsch, K. Klein, G. M. Kopper, W. J. Lauderdale, F. Lipparini, T. Metzroth, L. A. Mück, D. P. O'Neill, T. Nottoli, D. R. Price, E. Prochnow, C. Puzzarini, K. Ruud, F. Schiffmann, W. Schwalbach, C. Simmons, S. Stopkowicz, A. Tajti, J. Vázquez, F. Wang, J. D. Watts and the integral packages MOLECULE (J. Almlöf and P. R. Taylor), PROPS (P. R. Taylor), ABACUS (T. Helgaker, H. J. Aa. Jensen, P. Jørgensen, and J. Olsen), and ECP routines by A. V. Mitin and C. van Wüllen. For the current version, see **https://www.cfour.de** (last accessed 19 December 2023).

127 D. A. Matthews, L. Cheng, M. E. Harding, F. Lipparini, S. Stopkowicz, T.-C. Jagau, P. G. Szalay, J. Gauss and J. F. Stanton, *J. Chem. Phys.*, 2020, **152**, 214108.

128 M. V. Vener and J. Sauer, *J. Chem. Phys.*, 2001, **114**, 2623–2628.

129 J. S. Mancini and J. M. Bowman, *J. Chem. Phys.*, 2013, **139**, 164115.

130 T. J. Lee and P. R. Taylor, *Int. J. Quantum Chem.*, 1989, **36**, 199–207.

131 C. L. Janssen and I. M. B. Nielsen, *Chem. Phys. Lett.*, 1998, **290**, 423–430.

132 M. L. Leininger, I. M. B. Nielsen, T. D. Crawford and C. L. Janssen, *Chem. Phys. Lett.*, 2000, **328**, 431–436.

133 T. J. Lee, *Chem. Phys. Lett.*, 2003, **372**, 362–367.

134 P. Zielke and M. A. Suhm, *Phys. Chem. Chem. Phys.*, 2006, **8**, 2826–2830.

135 J. C. Howard, J. L. Gray, A. J. Hardwick, L. T. Nguyen and G. S. Tschumper, *J. Chem. Theory Comput.*, 2014, **10**, 5426–5435.

136 R. Hwang, S. B. Huh and J. S. Lee, *Mol. Phys.*, 2003, **101**, 1429–1441.

137 E. Miliordos and S. S. Xantheas, *J. Chem. Phys.*, 2015, **142**, 234303.

138 D. M. Bates, J. R. Smith, T. Janowski and G. S. Tschumper, *J. Chem. Phys.*, 2011, **135**, 044123.

139 T. H. Dunning Jr., K. A. Peterson and A. K. Wilson, *J. Chem. Phys.*, 2001, **114**, 9244–9253.

140 S. N. Johnson and G. S. Tschumper, *J. Comput. Chem.*, 2018, **39**, 839–843.

141 K. M. Dreux and G. S. Tschumper, *J. Comput. Chem.*, 2019, **40**, 229–236.

142 M. A. Perkins and G. S. Tschumper, *J. Phys. Chem. A*, 2022, **126**, 3688–3695.

143 M. A. Perkins and G. S. Tschumper, *Chem. Phys.*, 2023, **568**, 111843.

